



SOLAR WATER-HEATING DESIGN—A NEW SIMPLIFIED DYNAMIC APPROACH

P. T. TSILINGIRIS[†]

Centre for Renewable Energy Sources (CRES), 19th km Marathonos Avenue, 190 09 Pikermi, Attica, Greece

(Communicated by Doug Hittle)

Abstract—A simple computer simulation model suitable for the design of large solar water-heating systems has been developed. Compared with existing simplified correlation design methods, the present model allows a remarkable expansion of their applicability so as to incorporate any hourly demand profiles, solar system design configuration and heat losses from various system components, and remove any imposed restrictions referring to the definition range of the large number of design parameters involved. This flexibility is offered at no extra cost of complexity, long user experience and familiarity with the use of a complex computer code, something which is particularly important, especially for the practising solar designer or field engineer. Numerous results are presented referring to the effects of the variation of a broad range of main design parameters on system performance. The accuracy of the present model is validated against corresponding results from the familiar f-chart design method, the accuracy of which has been found to be very good according to comparisons between calculations and measured field data, as well as TRNSYS simulation results. Copyright © 1996 Elsevier Science Ltd.

1. INTRODUCTION

Proper large solar system design and typical annual thermal performance prediction are both issues of major concern for the promotion of large solar water-heating system technology in the potential market of large residential and hotel buildings, as well as in agriculture and the process industries.

Recent effort towards the elimination of user risks by means of a certain performance guarantee by the contractor, known as the “guaranteed performance” approach, is based on performance prediction modelling, which is carried out either by the simplified f-chart or by similar modified software versions. Aiming to relax several oversimplified assumptions usually made in most of the simplified solar system sizing tools, a new simple computer model has been developed to satisfy instructive and educational needs also. The effects of various system design and operational parameters, as well as heat losses from various system components and incidence angle modifiers for both the beam and diffuse radiation, have been investigated. Although thermal capacity effects of storage tanks have been properly accounted for in the calculations, the corresponding effects of solar collectors and interconnecting pipelines have been ignored. This assumption has an insignificant influence on the accuracy of the calculated

monthly and yearly results, owing to their appreciably smaller thermal capacity.

First results from an earlier version of the current improved model were previously reported by Tsilingiris (1993). The current version has been improved to incorporate, among other refinements, the separate treatment of direct and diffuse radiation through the introduction of appropriate incidence angle modifiers and the possibility of investigating the effect of hourly load profile on performance.

2. SOLAR SYSTEM DESIGN MODELLING

It is widely recognised that the most accurate and complete solar design tool currently available is the TRNSYS computer simulation model, developed by Klein *et al.* (1975). After its initial release 20 years ago, the numerical code has been very much enriched and refined and its validity and accuracy has been repeatedly confirmed, so it is broadly believed to be the best model currently available, mostly useful as an analysis and research tool. However, its widespread use is ruled out by cost, the relatively long user experience and appreciable expertise required to exploit the full model capabilities and the relatively complex meteorological data required.

Bearing this in mind and aiming at the development of a simple and low cost design tool, the simplified f-chart method was developed and proposed as early as 1976 (Klein *et al.*, 1976; Beckman *et al.*, 1977), based on the

[†]ISES Member. Correspondence address: 14 Th. Kairi str., Neasmirni, Athens 17122, Greece.

mathematical correlation of extensive computer simulation results by TRNSYS, in which conditions were varied over an appropriate range of system parameters involved. Results obtained by the f-chart method have been compared extremely well with the results from detailed simulations for a variety of geographical locations in both the USA and Europe. With the exception of a slight underprediction in cloudy climates, it was found by Evans *et al.* (1984), that the method predicted solar system performance with better than $\pm 5\%$ and as low as $\pm 2.2\%$ accuracy for space-heating and domestic solar water-heating systems, respectively.

The method offers serious advantages for the designer and field engineer, however it has many limitations, among which the specific design configuration, system size and design parameter restrictions, as well as the lack of flexibility to cover any hourly load demand profile, are most important.

From the time of its development, it was recognised that the complexity gap between detailed simulation models like TRNSYS and the f-chart correlation method was considerably wide and numerous attempts have been made to develop simplified methods of intermediate complexity level.

Among the most important is the development of the SOLCOST program by Colony *et al.* (1976), which models more solar system types and is somewhat more diverse than the early f-chart program versions. The model simulates a clear day and a cloudy day and then weights the results according to the average cloudiness to obtain a monthly estimate of system performance. It also allows thermal and economic analysis of combined heating and cooling systems and offers results which, according to Winn (1980), are within 6% of those from f-chart.

The Relative Areas method, originally proposed by Barley *et al.*, (1977), is based on correlation to results obtained by f-chart and it is offered for a quick and reasonably accurate calculation of the optimum collector area based on life cycle cost analysis. Derived results were found, according to Winn (1980), to be within 10% of those derived with f-chart.

The Solar Load Ratio (SLR) method was originally developed by Balcomb and Hedstorn (1976), to predict the monthly solar contribution of a solar heating system based on hour-to-hour simulations for 25 US locations and for five solar collector field sizes for each location.

The method offers comparable yearly results to those of f-chart.

More recently, another microcomputer model was reported by Schreitmuller (1988) that determines the holistic characteristics of a solar system for some typical days and uses these characteristics to determine the solar contribution to the load. The method was partly validated through simulations and field measurements, while further refinements, like solar collector field interconnecting network optimization and account of variation of thermophysical properties in the heat transfer loop, are on the way.

Guisan *et al.* (1988) have recently attempted to develop a very simple model suitable to predict the thermal performance of a solar system through hand calculations or a microcomputer. The aim of the model is the evaluation of the daily thermal output of a solar collector subsystem, composed of various collector types. Among the main assumptions are the constant daily load and ambient temperatures, ideal system regulation, sinusoidal variation of daily solar radiation and system temperature equal to ambient at the beginning of each day. The microcomputer version of the model includes a solar radiation generator routine operated through monthly or daily values, and refers to typical solar system configurations with storage tank, auxiliary heaters etc., while its validation against field measurements is claimed to be good.

The present work aims to describe a new computer model, suitable to carry out hourly simulation calculations throughout each successive month of the year, for the performance prediction and the operational behaviour investigation of solar water-heating systems, taking into consideration various component configurations and characteristics, control strategies, component heat losses and load demand profiles. Several of the f-chart simplified assumptions have been completely relaxed to extend remarkably the model applicability through user-friendly software code to any system configuration, design parameter and load profile, using very easily introduced meteorological data, which are appropriately processed to generate the required extensive data for the hourly calculations.

3. THE TYPICAL SYSTEM CONFIGURATION AND ASSUMPTIONS

Although several small, both free convection and forced circulation, domestic solar water-

heating systems are designed with a single, thermally stratified vertical storage tank with the solar heat exchanger immersed underneath the auxiliary heating coil, there is a general design trend for the provision of two separate tanks in larger solar water-heating systems. The first, usually called the solar tank (ST), is heated directly by solar energy as shown in Fig. 1. It is connected in series with the second, heated by the back-up auxiliary energy and usually called the auxiliary tank (AT). Both tanks are usually of standardized dimensions, installed horizontally in such a way that stratification effects are almost always minimized and can be completely ignored.

Recent developments indicate that a combination of appreciably lower mass flow rates at the collector loop of solar heating systems (as low as $0.002 \text{ l/m}^2 \text{ s}$) and thermally stratified tanks, mounted vertically and manufactured with specially designed baffles to eliminate mixing and improve stratification, may lead to, typically, as high as a 35% performance improvement. According to Hollands (1988), this system, known as the "low flow system", has been successfully demonstrated and appears to have potential for applications particularly in northern climates, while additional design refinements, mainly directed towards eliminating stagnation temperature conditions, are further required for application in sunny climatic conditions.

At its present state, the proposed model does

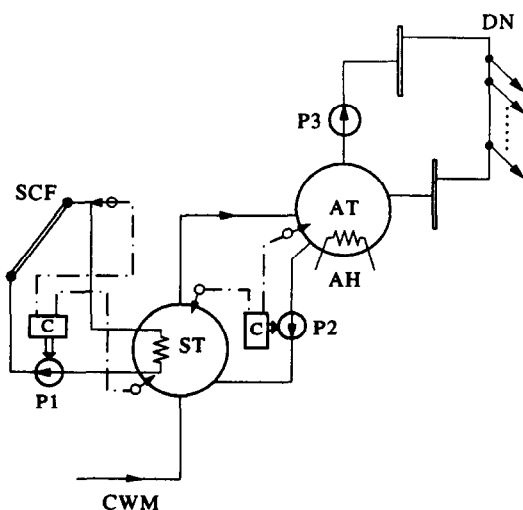


Fig. 1. The series connection of the solar preheating system tank ST with the afterheating tank AT in the investigated system design. SCF, the solar collector field; C, the controller; DN, the distribution network; CWM, cold water mains supply line.

not cover such low flow systems. Collector testing results according to the currently valid standard testing procedures (corresponding to higher mass flow rates typically between 0.01 and $0.02 \text{ l/m}^2 \text{ s}$) may be vastly different from those corresponding to low flow conditions. As soon as low flow collector testing data are available, they can be combined with a thermally stratified solar tank model to cover such systems, something which will be the aim of a further model refinement.

The cold water mains supply line (CWM) is connected to the ST (or to a bank of STs in even larger systems) and the hot water distribution network (DN) is connected to the AT. In closed-circuit systems, solar heat is transferred to the solar tank by circulation of antifreeze solution through an immersed coil, mantle or an external heat exchanger through the closed circuit pump P1. In open circuit systems the same pump P1 circulates the water directly to the collector field.

Pump P3 allows continuous hot water circulation in the "external" distribution hot water network. In addition to this, the "internal" circulation pump P2 is activated by an appropriate control device and transfers hot water to AT for immediate consumption, as soon as ST becomes higher than the AT temperature.

Both tanks are considered isothermal and a sufficient heat exchange rate in the solar collector closed-circuit loop ensures that the inlet collector field temperature is very close to ST temperature. Heat conduction losses from the distribution network and from the peripheral walls of both tanks are appropriately accounted for in the model, while the tank interconnection flow is assumed to be isothermal.

The default hourly hot water load profile throughout the day is assumed to be similar to Mutch (1974). However, owing to the fact that this assumption could only be adequately justified for most two daily peak domestic and sanitary water loads, it cannot cover the majority of other typical applications like industrial processes, greenhouse heating and any other single daily peak loads. Buckles and Klein (1980) have earlier simulated small domestic solar water-heating systems through TRNSYS to investigate the effect of collector area, tank size and insulation, tempering valves, as well as various hot water hourly load distribution profiles in the performance of single or double tank solar systems. The present model offers the possibility of investigating the effect of the daily

demand load profile and of incorporating, in addition to this, any other user specified daily load profile.

4. THEORETICAL ANALYSIS

4.1. The model description

The heat balance in the solar tank ST is given by the following expression:

$$\rho V_S c \frac{dT_S}{d\tau} = \frac{dQ_u}{d\tau} - \frac{dQ_w}{d\tau} + \dot{Q}_{RF} - \dot{Q}_S \quad (1)$$

where the left-hand side term corresponds to the sensible-heat storage in the solar tank and the four terms on the right-hand side of the above expression represent the rate of the net solar energy gain, the heating rate of the water outflow, the heating gain owing to the internal loop recirculation flow and the tank heat losses, respectively.

The net solar heat gain is given by:

$$\frac{dQ_u}{d\tau} = A_c F_R (F'_R/F_R) [S - U_L (T_i - T_a)] \quad (2)$$

where (F'_R/F_R) is the collector-heat exchanger factor which represents the penalty in solar collector gain owing to the introduction of the heat exchanger at the closed-circuit loop. Solar energy absorption S is given by:

$$S = (\tau\alpha)_n \left(R_b I_b K_b + I_d K_d \frac{1 + \cos \beta}{2} + (I_b + I_d) r_g K_g \frac{1 - \cos \beta}{2} \right) \quad (3)$$

where the incidence angle modifier for the direct component of solar radiation is given by:

$$K_b = 1 + b_0(1/\cos \theta_{eb} - 1) \quad (4)$$

θ_{eb} , the incidence angle of the beam solar radiation, and the numerical constant $b_0 = -0.1$ is for single glazed collectors. For the sky and ground diffuse radiation, this coefficient is given as a function of the diffuse radiation equivalent sky and ground incidence angles:

$$K_d = 1 + b_0(1/\cos \theta_{ed} - 1) \quad (5)$$

$$K_g = 1 + b_0(1/\cos \theta_{eg} - 1) \quad (6)$$

The equivalent sky and ground incidence angles for diffuse radiation are given as a function of the collector field tilt angle, and calculated according to Duffie and Beckman (1980):

$$\theta_{ed} = 59.68 - 0.1388\beta + 0.001497\beta^2 \quad (7)$$

$$\theta_{eg} = 90 - 0.5788\beta + 0.002693\beta^2 \quad (8)$$

The water heating rate is given by:

$$\frac{dQ_w}{d\tau} = \rho \dot{V} c (T_S - T_G) \quad (9)$$

where \dot{V} is the volumetric flow rate of water. The heating rate owing to the "internal" recirculation flow is:

$$\dot{Q}_{RF} = \rho \dot{V}_{RF} c (T_A - T_S) \quad (10)$$

where \dot{V}_{RF} is the volumetric recirculation flow rate given by

$$\dot{V}_{RF} = \min(V_S, V_A)/\Delta T \quad (11)$$

ΔT is the selected time step during the integration throughout the period of calculation, and the solar tank heat losses are given by:

$$\dot{Q}_S = A_S U_S (T_S - T_R) \quad (12)$$

where A_S is the solar tank heat transfer area, given as a function of its volume capacity.

The heat balance in the auxiliary tank is given by:

$$\rho V_A c \frac{dT_A}{d\tau} = P_A - \dot{Q}_A - \dot{Q}_{RF} - \frac{dQ_{L0}}{d\tau} \quad (13)$$

where the four terms on the right-hand side of the heat balance correspond to the auxiliary input heating rate, heat losses from auxiliary tank, heating rate owing to internal recirculation and load. The auxiliary heating power is so selected as to satisfy the hourly maximum daily hot water demand load:

$$\dot{Q}_A = \lambda \max(\dot{V}) \rho c (T_{ws} - T_G) \quad (14)$$

Auxiliary heater capacity is determined by the hourly peak hot water demand, $\max(\dot{V})$ and the supply temperature and λ is a safety margin numerical constant taken to be $\lambda = 1.3$.

As soon as the AT temperature becomes lower than the predetermined hot water supply temperature, the thermostatically controlled auxiliary heater goes on to top up the supply temperature to the desired level.

The heat loss from the auxiliary tank is given by:

$$\dot{Q}_A = A_A U_A (T_A - T_R) \quad (15)$$

where A_A is the auxiliary tank heat transfer area.

The final load term is expressed as a contribution of two load components, the heating water and the distribution network load component, respectively:

$$dQ_{L0}/d\tau = dQ_{Lw}/d\tau + dL_{L1}/d\tau \quad (16)$$

where

$$dQ_{Lw}/d\tau = \rho \dot{V} c (T_L - T_S) \quad (17)$$

and

$$dQ_{L1}/d\tau = h_{ds}L(T_A - T_R) \quad (18)$$

4.2. The meteorological data input

The aim of computer simulation calculations is the thermal performance and operational behaviour prediction of a solar system under the influence of typical climatological conditions for the specific geographical site. Owing to the stochastic nature of these data, the reliability of the calculated results depends on how accurately they reproduce the typical local climate. It is clear that unusual measurements corresponding to scarce weather phenomena would be possible in a set of short-term measurements, and in this case their effect could strongly affect the accuracy of the calculated typical system performance and thermal behaviour. However their influence will be gradually smoothed out as soon as the time series of the available data becomes longer.

The selection of the appropriate meteorological data input for the investigation of the system response under the influence of these time-dependent forcing functions to the mathematical models of all system components, is a very crucial factor for the prediction of typical system behaviour.

Usually owing to the lack of long-term measurements, various investigators have been led to select a particular year, which appears to be typical, from a few years of data. In an attempt to use typical weather in his simulations, Klein *et al.* (1975), have selected each typical month of his typical year on the basis that the selected month had the same mean radiation as the mean of that month calculated from 10 years of data. Relevant work has been carried out by Benseman and Cook (1969) and Petrie and McClintock (1978). Extensive test reference-years data in a computerized form corresponding to a few European locations have been also reported by Lund (1985).

Current work is based on a statistical treatment of a rather long sample of some 25 years of solar radiation data from the National Observatory of Athens and on over 20 years of ambient temperature data from the National Meteorological Service corresponding to the Athens area, by Kouremenos and Antonopoulos (1985) and Kouremenos *et al.* (1985). Hourly solar insolation measurements carried out over the period 1961–1980 were integrated over all hours of the day to derive the daily values of

the average total solar radiation incident at a horizontal surface and were fitted by simple harmonic functions for the direct calculation of the daily average solar radiation at the horizontal surface. The accuracy of this mathematical fit for the given site is expected to be a function of the number of the harmonic terms. It was found by Kouremenos and Antonopoulos (1985) that, for the particular geographical location, very good accuracy (within 5%) can be obtained with a single harmonic term.

Monthly average solar radiation figures derived from those measurements have also been found to be in good agreement with relevant data from relative investigations by Lalas *et al.* (1982), for the same geographical region.

Calculation of the long-term daily average temperatures is possible by the integration of the corresponding long-term hourly measurements. However, owing to the lack of such long-term detailed hourly data, it was found (Kouremenos *et al.*, 1985) that good approximation of the daily average temperature figures for the given geographical site can be derived by simply averaging the available measured daily maximum and minimum temperatures for the period of the years 1950–1975. The calculated results were employed to derive long-term daily range, maximum and average temperatures for each day of the year and were fitted with a good accuracy by harmonic functions. The so-derived daily data were employed for the calculation of hourly average ambient temperature throughout the day, according to the model proposed by ASHRAE (1981).

The time scale of the employed data is considered adequately long to smooth out appropriately any unusual climatic extremes and meteorological events. All these hourly solar radiation and ambient temperature data are derived and stored for the daily sequence of calculations throughout each month of the year.

It appears as though the same procedure can also be easily adapted for other geographical locations of interest, as soon as there is access to long-term daily measurements of solar radiation and ambient temperature for the particular location.

4.3. The computer model

As soon as eqns (1)–(18) were translated to their finite-difference form, user-friendly computer software code was developed to carry out sequential calculations through an appropriate time step ΔT , for the entire time domain of each

month of the year. For simplicity and in order to maintain a reasonably short monthly integration time, it was found convenient to select hourly time steps throughout integration. Various additional system design variables are then introduced, such as collector testing parameters $F_R \cdot (\alpha\tau)_n$ and $F_R \cdot U_L$, tank capacities, loss coefficients, specific hourly demand profiles, etc. The extensive hourly solar radiation data required for the calculations are then generated by the computer model from corresponding long-term daily average data. These are introduced very easily in the form of a simple harmonic mathematical fit, corresponding to long-term daily average total solar radiation data incident at a horizontal surface and they are split subsequently into daily direct and diffuse components, according to the Liu and Jordan (1960) procedure. Then the hourly total, direct and diffuse components are calculated according to relevant standard procedures, as described by Duffie and Beckman (1980). Hourly values of incidence and zenith angles for the beam solar radiation are then calculated for the evaluation of the beam solar radiation at any tilt and azimuth angle of the collector field.

The simulation begins as soon as initial temperatures T_s and T_l at the beginning of each month (first hour of the first day of the month) are defined, the computer model calculates and stores the hourly load demand and the solar heat gain.

The monthly heating load and solar contribution are calculated, respectively, by:

$$Q_{LM} = \sum_{j=1}^N \sum_{k=1}^{24} (dQ_{L0}/d\tau) \Big|_{j,k} \quad (19)$$

$$Q_{uM} = \sum_{j=1}^N \sum_{k=1}^{24} (dQ_u/d\tau) \Big|_{j,k} \quad (20)$$

where N is the number of days of the particular month.

The calculated monthly and yearly solar fraction is given by the following two expressions, respectively:

$$MSF = Q_{uM}/Q_{LM} \quad (21)$$

$$YSF = \frac{\sum_{m=1}^{12} \sum_{j=1}^N \sum_{k=1}^{24} (dQ_u/d\tau) \Big|_{k,j,m}}{\sum_{m=1}^{12} \sum_{j=1}^N \sum_{k=1}^{24} (dQ_{L0}/d\tau) \Big|_{k,j,m}} \quad (22)$$

5. RESULTS AND DISCUSSION

In Fig. 2 the yearly solar fraction is plotted as a function of collector field area. Both solid lines correspond to a system of a fixed solar storage tank capacity to collector field area ratio, equal to $(V_s/A_c) = 50 \text{ l/m}^2$. It is shown that for the specific system of about 90 m^2 a yearly solar fraction of about 40% is possible. Both solid lines are also offered for comparative investigation of the effect of the internal recirculation flow through pump P2 on yearly performance. It is shown that the system design without the internal recirculation flow loop ($RF = 0$) leads to a lower yearly performance. The calculated higher yearly solar fraction corresponding to the particular system, which includes the combination of P2 pump and associated controller, leads to a higher solar fraction.

Distribution network losses corresponding to an average pipe network length of 350 m are assumed throughout and the broken line corresponds to operation with fixed solar tank capacity of 3000 l and internal recirculation flow ($RF = 1$).

It is also shown that operation with a fixed solar tank capacity of 3000 l and $RF = 1$ leads to a very slightly higher than constant performance for small collector field areas. At larger collector field areas and for storage-capacity-to-collector-area ratios lower than 50 l/m^2 , there is a comparatively slight decrease of performance, although the operational modes corresponding to constant volume-to-area ratio and constant volume of 3000 l lead to comparable yearly performances.

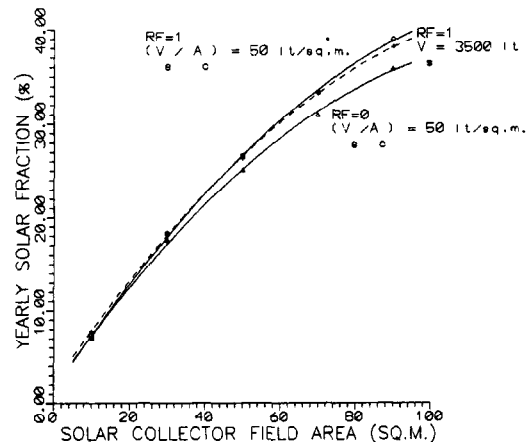


Fig. 2. Yearly solar fraction as a function of solar collector area. Solid lines correspond to a system design with recirculation flow through pump P2 ($RF = 1$) and without this flow ($RF = 0$). Broken line corresponds to constant solar tank capacity and $RF = 1$.

The effect of collector field tilt angle on the yearly solar fraction for a fixed solar collector field area of $A_c = 70 \text{ m}^2$ is shown in Fig. 3. Plotted results correspond to a fixed solar-tank-capacity-to-collector-area ratio of 50 l/m^2 , $RF = 1$ and an average distribution network length of 350 m . It is shown that although the yearly performance is only slightly affected by this parameter for values up to 45° it declines significantly at higher values of the tilt angle.

The effect of the solar tank capacity on yearly solar fraction is shown in Fig. 4 for a fixed solar collector area of 70 m^2 , $RF = 1$ and $L = 350 \text{ m}$. Both storage-tank heat-transfer area and thermal insulation effectiveness have been employed for the evaluation of tank heat losses. Storage-tank heat-transfer area has been assumed to be a function of storage capacity according to the

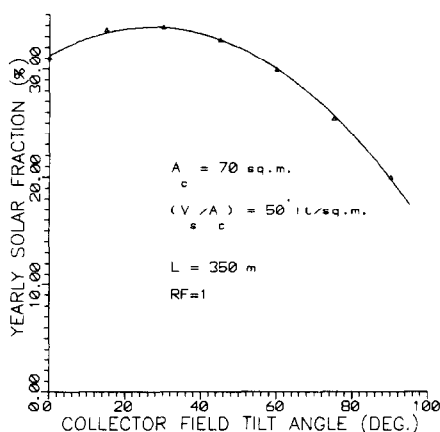


Fig. 3. Yearly solar fraction as a function of collector field tilt angle for a fixed collector area system of 70 m^2 , $RF = 1$ and storage-capacity-to-collector-area-ratio equal to 50 l/m^2 .

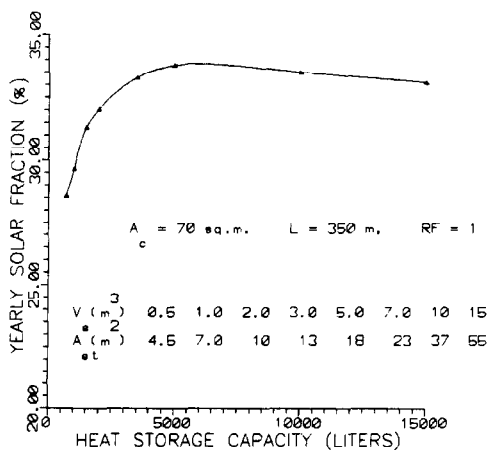


Fig. 4. The effect of solar heat storage capacity to yearly solar fraction for a fixed collector field area of 70 m^2 and $RF = 1$.

typical numerical figures shown in the legend contained in Fig. 4. Linear interpolation has been employed for sizes not included within the whole investigated capacity range.

It can be seen that the increasing effect of storage capacity on the yearly performance for about the first 3000 l is very strong. For higher capacities there is a further, although slower, yearly solar fraction increase, with a maximum nearly at 5000 l . Although an even far slower performance increase would be expected for even larger storage tanks, the opposite effect is observed for capacities up to $15,000 \text{ l}$. This is attributed to the effect of excessive heat losses from the peripheral wall of the storage tanks on performance as soon as they become very large. Heat losses are proportional to the heat-transfer area and their negative effect on yearly solar fraction is comparatively stronger than the corresponding performance contribution owing to storage-tank capacity increase.

Owing to the need to provide hot water throughout the day in most large commercial and residential buildings, continuous hot-water circulation flow through long distribution networks is usually necessary. Distribution heat losses then usually represent a significant fraction of the combined water heating and distribution loss load, the relative significance of which, as compared to water-heating load on yearly performance, is shown in Fig. 5. In this plot the comparative yearly solar fraction is shown as a function of collector field area for two solar systems with identical water-heating load, although with a completely different distribution network load. The first corresponds to a system design without a distribution network $L = 0$,

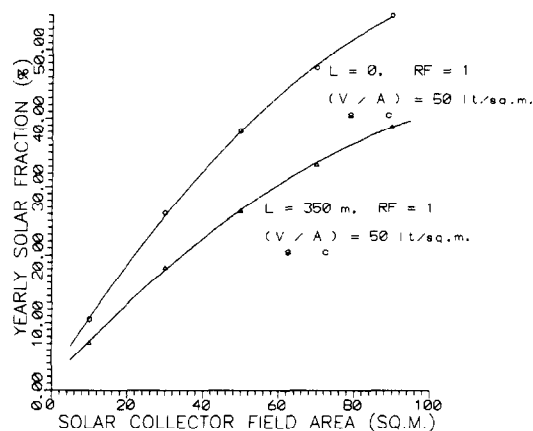


Fig. 5. The effect of distribution heat loss load component on yearly solar fraction for a fixed solar-tank-capacity-to-collector-area ratio of 50 l/m^2 and $RF = 1$.

while the second corresponds to a typical distribution network of 350 m long. The significance of proper thermal insulation and the reduction or complete elimination of heat losses is shown, since complete elimination of the distribution network leads to typically about a 30% increase of yearly solar fraction for the whole investigated range of solar collector areas.

The comparative effect of the hourly hot-water demand profile on the yearly solar fraction is shown in Fig. 6. To allow direct comparisons that are solely due to the effect of completely different water consumption profiles, the additional distribution heat-loss load component is ignored ($L = 0$) and three more normalized hourly water-consumption profiles have been introduced into the computer model, as shown in Fig. 7. The duration of all three profiles is 4 h daily, with the evening peak between 6 pm and 9 pm, the midday peak between 12 am and 3 pm and the morning peak between 6 am and 9 am, corresponding to profiles 1–3 of Fig. 7, respectively. In the same plot, the familiar twin peak hourly demand is also shown by line 4.

The solid lines shown in Fig. 6 correspond to the three peak demand profiles, while the broken line corresponds to the normalized Much profile, as shown in Fig. 7. It can be seen that the midday peak profile leads to about 15% higher than both evening and morning peak yearly solar fractions, owing to the good coincidence of maximum solar radiation with the load demand, especially at larger collector field areas. It leads also to appreciably higher yearly solar fraction than the corresponding Much profile performance. Yearly solar fraction correspond-

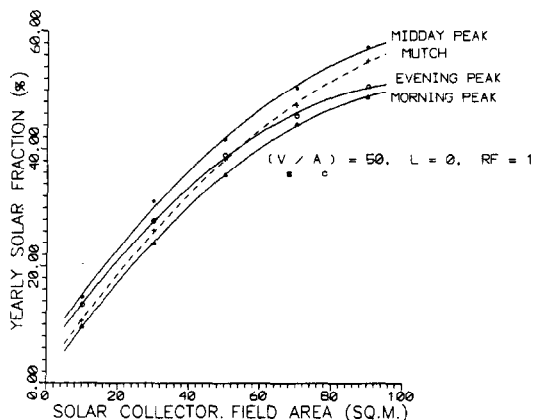


Fig. 6. The effect of hourly hot water demand profile on a yearly performance as a function of solar collector area for constant solar-tank-heat-storage-capacity-to-collector-area equal to 50 l/m^2 , $RF = 1$ and no distribution loss load component, $L = 0$.

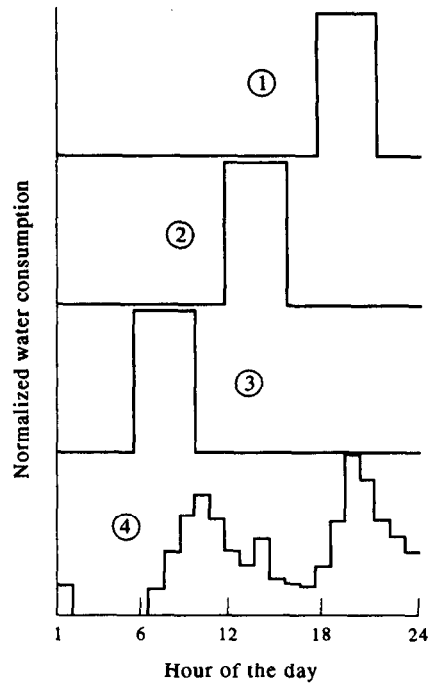


Fig. 7. The form of the four normalized water consumption profiles throughout the presented results of calculations. Profiles 1–3 correspond to the evening, midday and morning peak demand, respectively, while profile 4 corresponds to the domestic daily consumption profile according to Much.

ing to the Much (1974) and evening profiles shows a comparable solar fraction, especially at collector field areas between about 30 and 70 m^2 . Morning peak profile leads to even lower performance owing to the excessive storage losses throughout most of the day, due to the appreciable time lag between peak solar radiation and load demand.

6. COMPARISON WITH SIMPLIFIED ANALYSES

The f-chart procedure is believed to be the most popular and widespread simplified solar system design method. Although comparisons between yearly solar fractions calculated by f-chart and accurate computer simulations by TRNSYS have shown excellent agreement, they have been found to be not as good for monthly solar fractions and therefore f-chart use has been recommended only for the estimation of annual performance by Duffie and Beckman (1980). Its accuracy has been found to be the matter of long, sometimes conflicting debates over the last 20 years. Its validity has earlier been found to be under question several times, owing to the inherent simplifications and the limited database for comparisons with measured

data. Reports have also sporadically appeared in the literature regarding the degree of user confidence, especially for applications over a wide range of climatic conditions (Duffie *et al.*, 1977).

For several years only a limited database of measured performance has been available to allow for general comparisons between measured and predicted performance. However, as the time went by, more and more comparative reports have appeared in the scientific literature, supporting a growing degree of confidence in this simplified method, which, according to Duffie and Mitchell (1983), has been found to offer agreement between measurements and predictions up to within $\pm 3\%$. This degree of confidence, which is good for a simplified design method, is now widely accepted (Evans *et al.*, 1984). The method is now accepted as being applicable over a wide range of climatic conditions and for this reason a comparison between the results given by f-chart and by the proposed design method would be of considerable interest.

The present model has been used to calculate the monthly and yearly solar fractions of a particular solar system with a collector area of 10, 30, 50, 70 and 80 m², serving a heating load of 6000 l/day with a demand profile corresponding to Mutch, storage capacity to collector area of 50 l/m² and negligible distribution heat losses, $L = 0$. Monthly average values of the meteorological data input in the present computer model are employed as input data for the latest version 5 of the f-chart software, which has been made available by its original developers, the F-Chart Software company.

Although monthly solar fraction comparisons between f-chart and the present model should be made without much confidence, there is fairly good agreement between most monthly results, although the scatter around the unity slope line is rather wide, as shown in Fig. 8. It is shown that the majority of monthly derived results compare very well, although appreciable deviations are observed for certain months of the year. More specifically, up to 25% higher monthly solar fraction is predicted by the present model for July and September and the model underestimates considerably the performance for October. The comparative prediction between yearly solar fractions is shown in the same plot, corresponding to the large crossed-circle data points. The yearly solar fraction data points, according to the present model, are compared with the f-chart results, there is a

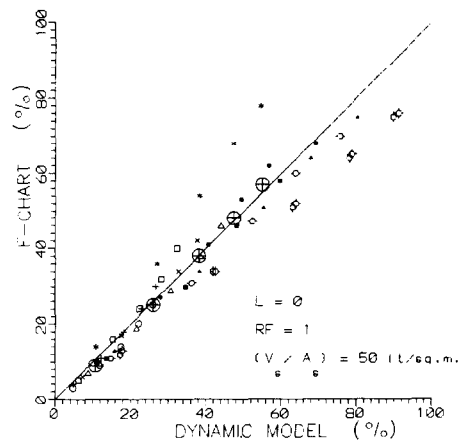


Fig. 8. Comparative presentation of results from the present dynamic model and f-chart correlation model calculations. Large crossed-circle point data correspond to derived yearly results. Small data points correspond to the following months: \circ January, \square February, \triangle March, \bullet April, \blacksquare May, \blacktriangle June, \diamond July, \ominus August, \odot September, $*$ October, \times November, $+$ December.

little scatter around the unity slope line, indicating very good agreement between results from the present model and f-chart method.

7. CONCLUSIONS

A computer model suitable for solar system performance predictions and operational behaviour investigations has been developed. The model, which can readily be used in a conventional microcomputer, is a powerful solar system design tool and is suitable to carry out extensive hourly calculations for each month of the year, based on easily introduced and broadly accessible meteorological data. The use of the present model allows relaxation of many of the simplifying assumptions and restrictions imposed by the use of the simplified f-chart design method, as based on the correlation of results by the more powerful and highly advanced computer simulation code TRNSYS. The background theoretical analysis has been presented along with typical derived results, referring to the effect of the main system parameter variation on the load fraction supplied by solar energy. Comparative presentation of the derived results shows very good agreement between the present model and the f-chart correlation method.

NOMENCLATURE

- A surface (m²)
- b_0 numerical constant
- c specific heat capacity (J/kg C)
- F_R collector heat removal factor

(F_R/F_{Rc}) collector-heat exchanger factor
 h average unit length heat loss coefficient (w/m C)
 j number of day of the month, $1 \leq j \leq N$
 k number of hour of the day, $1 \leq k \leq 24$
 K incidence angle modifier
 L length (m)
 m number of month of the year, $1 \leq m \leq 12$
MSF monthly solar fraction
 N number of days per month
 Q energy (J)
 \dot{Q} energy rate (w)
 r reflectivity
 R geometric factor
 T temperature ($^{\circ}\text{C}$)
 S solar energy absorption rate (W/m^2)
 U heat loss coefficient ($\text{W}/\text{m}^2\text{ }^{\circ}\text{C}$)
 V volume (m^3)
 \dot{V} volume flow rate (m^3/s)

Greek letters

β collector field tilt angle ($^{\circ}$)
 ΔT time step (s)
 θ incidence angle ($^{\circ}$)
 λ numerical constant
 ρ density (kg/m^3)
 $(\tau\alpha)$ transmittance-absorbance product
 τ time (s)

Subscripts

a ambient
 A auxiliary tank
 b beam
 c collector
 d diffuse
 ds distribution
 eb equivalent beam
 ed equivalent diffuse
 eg equivalent ground
 g ground
 G groundwater
 i inlet
 L loss
 Ll load component due to distribution losses
 LM monthly load
 Lw load component due to water heating
 $L0$ sum of load components
 n normal
 R boiler room
 RF recirculation flow
 S solar tank
 th thermostat
 u useful
 uM monthly useful
 w water
 ws water supply

REFERENCES

- ASHRAE (1981) Air conditioning cooling load. In *The Handbook of Fundamentals*. ASHRAE, New York. pp. 26.1–26.46.
- Balcomb D. J. and Hedstorn J. C. (1976) A simplified method for calculating solar collector array size for space heating. *Proc. Joint AS/ISES and Solar Energy Society of Canada Conf.*, Vol. 4, Winnipeg, Canada, pp. 220–234.
- Barley C. D. and Winn C. B. (1977) The relative areas method for optimal collector sizing of solar systems. Solar Energy Applications Laboratory, Colorado State University, Ft. Collins, CO.
- Beckman W. A., Klein S. A. and Duffie J. A. (1977) *Solar Heating Design by the f-chart Method*. Wiley Interscience, New York.
- Benseman R. F. and Cook C. F. (1969) Solar radiation in New Zealand: the standard year and radiation on inclined slopes. *NZ J. Sci* **12**, 696–704.
- Buckles W. E. and Klein S. A. (1980) Analysis of solar domestic hot water heaters. *Solar Energy* **25**, 417–424.
- Collony M., Giellis R., Jensen C. and McMordie R. (1976) Solar heating and cooling analysis—a simplified sizing design method for non-thermal specialists. *Proc. Joint AS/ISES and Solar Energy Society of Canada Conf.*, Vol. 10, Winnipeg, Canada, pp. 220–234.
- Duffie J. A., Beckman W. A. and Decker J. G. (1977) Solar heating in North America. *Mech. Engng* **99**(11), 37–45.
- Duffie J. A. and Beckmann W. A. (1980) *Solar Engineering of Thermal Processes*. John Wiley, New York, pp. 67–83, 505–506.
- Duffie J. A. and Mitchell J. W. (1983) f-Chart: predictions and measurements. *J. Solar Energy Engng* **105**, 3–9.
- Evans B. L., Beckman W. A. and Duffie J. A. (1984) f-Chart in European climates. *Proc. 1st Eur. Conf. Solar Heating*, Den Ouden C. (Ed.), Amsterdam, pp. 161–165.
- Guisan O., Lachal B., Mermoud A. and Rudaz O. (1988) G3 model: a simple model for the evaluation of the thermal output of a solar collection system on a daily basis. *Proc. ISES Solar World Congress*, Hamburg.
- Hollands K. G. T. (1988) Recent developments in low-flow stratified-tank solar water heating systems. *Proc. North Sun 88 Conf.*, Swedish Council of Building Research, Borlange, Sweden, pp. 101–110.
- Klein S. A., Cooper P. I., Freeman T. L., Beckman D. M., Beckman W. A. and Duffie J. A. (1975) A method of simulation of solar processes and its application. *Solar Energy* **17**, 29–35.
- Klein S. A., Beckman W. A. and Duffie J. A. (1976) A design procedure for solar heating systems. *Solar Energy* **18**, 113–127.
- Kouremenos D. A., Antonopoulos K. A. and Domazakis E. S. (1985) Solar radiation correlations for the Athens, Greece area. *Solar Energy* **35**, 259–269.
- Kouremenos D. A. and Antonopoulos K. A. (1985) Ambient temperature correlations in 35 locations in Greece (in Greek). Fivos edn, Athens.
- Lalas D. P., Pissimanis D. K. and Notaridou V. A. (1982) Methods for estimation of the intensity of solar radiation on tilted surface and tabulated data for 30, 45 and 60 deg. in Greece. *Tech. Chron. Section B* **2**(3,4), 129–178.
- Liu B. Y. and Jordan R. C. (1960) The interrelationship and characteristic distribution of direct, diffuse and total solar radiation. *Solar Energy* **4**(3), 1–19.
- Lund H. (1985) *Test Reference Years*. TRY, CEC-DGXII, Brussels.
- Mutch J. J. (1974) Residential water heating, fuel consumption, economics and public policy. RAND Report R1498.
- Petrie W. R. and McClintock M. (1978) Determining typical weather for use in solar energy simulations. *Solar Energy* **21**, 55–59.
- Schreitmuller K. R. (1988) Modelling of active solar energy systems with holistic characteristics. *Proc. ISES Solar World Congress*, Hamburg, pp. 828–835.
- Tsilingiris P. T. (1993) A flexible simulation model for use in solar central water heating systems. *Proc. ISES Solar World Congress*, Vol. 5, Kabloody E. (Ed.), Budapest, Hungary, pp. 151–156.
- Winn C. B. (1980) Solar simulation computer programs. In *Solar Energy Technology Handbook, Part B*, Dickinson W. C. and Cheremisinoff P. N. (Eds). Marcel Dekker, New York, pp. 481–515.